International Journal of Fracture **125:** 33–50, 2004.

Numerical analysis of the effect of microstructures of particle-reinforced metallic materials on the crack growth and fracture resistance

L. MISHNAEVSKY JR[1,2], U. WEBER[1] and S. SCHMAUDER[1]
[1] *University of Stuttgart, IMWF (Institute of Materials Testing, Materials Science and Strength of Materials), Pfaffenwaldring 32, D-70569 Stuttgart, Germany*
[2] *Institute of Mechanics, AG IV, Darmstadt University of Technology, Hochschulstrasse 1, 64289 Darmstadt, Germany (E-mail: mishnaevsky@web.de)*

Received 11 November 2003; accepted 14 November 2003

Abstract. This paper presents a systematical computational study of the effect of microstructures of materials reinforced with brittle hard particles on their fracture behavior and toughness. Crack growth in particle-reinforced materials (here, in high speed steels) with various artificially designed arrangements of brittle inclusions is simulated using microstructure-based finite element meshes and an element elimination method. The following types of brittle inclusions arrangements are considered: (simple microstructures) net-like continuous, band-like, random with different inclusion sizes, and (complex microstructures) layered and clustered arrangements, with different inclusion sizes and orientations. Crack paths, force-displacement curves, fracture toughness and fractal dimension of fracture surfaces are determined numerically for each microstructure of the materials. It is demonstrated that extensive crack deviations from the initial cracking directions and an increase in the fracture toughness can most efficiently be achieved by using complex microstructures, such as alternated layers of fine and coarse inclusions.

1. Introduction

This paper presents a systematic computational study of the effect of microstructures of metallic materials reinforced with brittle hard particles on their fracture behavior and toughness. Various material microstructures are tested numerically under the same loading conditions. The value of numerical experiments in predicting and improving material performance is demonstrated using the example of high speed steels.

The optimal design of particle-reinforced materials on the basis of computational simulations of their behavior has attracted growing interest of researchers over the last two decades (Mishnaevsky and Schmauder, 2001; Mishnaevsky et al., 1999, 2003a,b). The computational design of materials for industrial needs is possible, if the computational difficulties concerning simulation of complex materials at many scale levels are resolved and corresponding technologies for the creation of the materials are available. Steels are among the group of most investigated materials in the world, and have widely been used industrially in many centuries. Among them, tool steels hold a special position, both due to their wide use in the metal-working industry, and due to the complex requirements on their properties: the microstructure of a tool steel must ensure high hardness and wear-resistance (these properties of tool steels are secured by the availability of hard and brittle primary carbides in the materials), as well as high fracture toughness and lifetime (which are influenced by the properties of the 'matrix' of the steels, and the secondary carbides) (Mishnaevsky et al., 2001b,c; Le Calvez et al., 2000; Berns

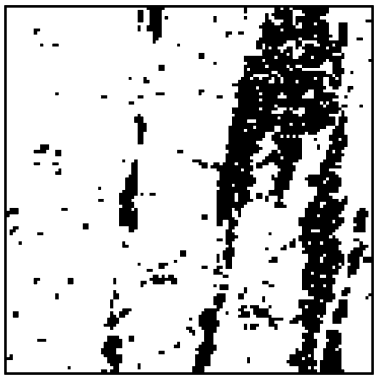

Figure 1. Discretized micrograph of high speed steel HS6-5-2 (Mishnaevsky et al., 2003b). The black areas represent primary carbides, the white area is the 'matrix'. Region dimension 100 μm $\times$ 100 μm.

et al., 1997, 1998). On the other hand, microstructures of tool steels can be altered by using different technologies (casting, powder metallurgy, different heat treatment and working), and, therefore, the recommendations to be developed here can be practically realized (Le Calvez, 2000). That is why we chose tool (high speed) steels as an object for the computational testing of artificially designed microstructures, and analysis of microstructurefracture resistance relationships. A further reason for the choice of steels as a test object for the computational testing of microstructures is that microcracks initiate in primary carbides in the steels (Mishnaevsky et al., 2001a,b, 2003); therefore, the initial distribution of primary carbides corresponds to the distribution of potential sites of the crack initiation. Table 1 gives a short review of the micromechanical studies of the interrelations between the structure and fracture resistances of tool steels.

This study presents a continuation and development of previous work by the authors (Mishnaevsky et al., 2001, 2003a,b), in which the effect of different arrangements of brittle inclusions on the fracture resistance was considered. As differentiated from our previous works, we concentrate here on the study of 'complex' microstructures; i.e. microstructures which consist of regions with different particle densities or different particle sizes.

2. Numerical methods of the analysis of microstructures in the mechanics of materials

Microstructure modeling at the level of Gaussian points and at finite element level

Information about the microstructure of a material is usually given as a 2D (discretized) micrograph (or, in 3D case, as a series of micrographs) (Mishnaevsky et al., 1999; Schmauder and Mishnaevsky, 2001). Figure 1 shows a discretized micrograph of high speed steel HS6-5-2 used in real structure simulations (Mishnaevsky et al., 2003a).

In order to include the microstructure information in the FE model, there exist in general two methods: first, to impose the complex microstructure on a simple FE mesh without adapting the mesh to the microstructural phase boundaries and second, producing a FE mesh according to the microstructure of the micrograph.

The automatic assignment of the digitised microstructure to a simple FE mesh can be done in the framework of multiphase finite elements (MPE) (Figure 2) (Mishnaevsky and

Table 1. Some research works in the area of the strength and fracture of tool steels

Authors, steel type	Numerical approach, codes	Problems and Main results
Plankensteiner et al. (1996, 1998). Steel: Electroslag remelted HSS, with netlike carbide arrangement	PATRAN, ABAQUS. Mesophase Cell Hierarchical Modeling (this approach includes unit cell technique, and transformation field approach or incremental Mori-Tanaka approach).	Overall response of steels as well as mechanisms of local failure in steels with real structures are studied. The effect of progressive carbide cleavage on the stressstrain curve is considered. Stress-strain curves, and distributions of maximum principal inclusion stresses are obtained. It is shown that the carbide grain cleavage is a main fracture mode at microscale.
	HEXGRAIN, ABAQUS. Hexagonal Cell Tiling Concept (unit hexagonal cells containing a number of inclusions).	Stress distribution, and also an effect of initial thermal residual stresses on the parameters of stress distribution are considered. Stress level within carbide particles and in matrix, and the effect of thermal stresses on them are studied.
Broeckmann (1994). Steels: Ledeburitic chromium steel SAE-D3 in as cast condition and hot worked state	CRACKAN. Modeling of real structures. Plasticity of matrix is modeled with J2 flow theory. Carbide particles fail due to cleavage along crystallographic planes.	Influence of carbide particle distribution on the fracture processes in steel is investigated. Stress distribution in real microstructure ahead of main crack, local damage and effect of local triaxiality on cleavage strength of carbides are studied.
Gross-Weege et al. (1996). Steel: as above; HSS manufactured by powder metallurgy and HIP	CRACKAN (like above). Decohesion between carbides and matrix occurs if the stresses normal to the interface reach a critical value. Unit cell model is used to study the interaction between inclusions.	Simulation of crack initiation (also in front of main crack) due to particle cracking and interfacial failure. Particle cracking, damage evolution in front of main crack are studied.
Lippmann et al. (1996). Steel: Electroslag remelted HSS, with 50% hot reduction	ANSYS. Crack faces are predefined with the use of nonlinear spring elements	Crack initiation by carbide failure is simulated. Crack distribution in real structure of steel. It is shown that long and thin carbides fail first and form initial cracks.
	LARSTRAN. Method of multiphase elements (MPE) makes possible to simplify preprocessing. Automatic element elimination technique is used to model crack initiation and growth.	Crack initiation, growth and distribution in real structure of HSS. Stress and crack distribution in real structures is obtained; effect of carbide stringer width of the crack formation is studied.

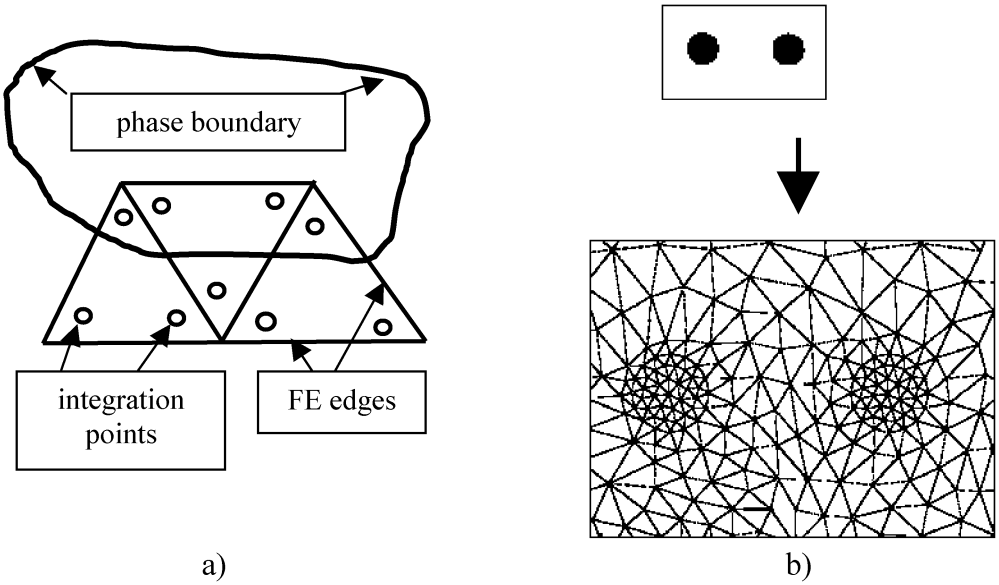

Figure 2. Schemes: Multiphase finite elements (a) and automatic FE mesh generation from microstructures (b)

Schmauder, 2001; Mishnaevsky et al., 1999). The main feature of this method is that the different phase properties are assigned to individual integration (Gaussian) points in the element. Contrary to traditional (single-phase) finite elements, a FE-mesh is independent of the phase structure of material in this case, and relatively simple FE-meshes can be used for the simulations of the deformation in a complex microstructure. The possibility of using FE meshes of arbitrary simple structures for the simulation of the behavior of complex materials is the main advantage of the method of multiphase elements. Therefore, a relatively simple simulation of material behavior in the 3D case becomes possible. One should note however that MPE do not allow one to take into account local effects of interfaces. In some cases this limitation can be useful in order to help to reflect better the gradual transition of the local material properties. In the cases of materials in which neither phase is soluble in any other phases, the interface presents a real boundary and the impossibility taking into account interface effects using MPE can present a serious limitation for the MPE applicability.

Another approach is to produce a FE mesh which corresponds to a given microstructure. The main idea of this approach is that a FE mesh is automatically generated in such a way that the boundaries of 'surfaces' correspond to the phase boundaries in digitized microstructure micrographs. At the MPA Stuttgart a series of programs was developed, which allow one to generate automatically a FE mesh in PATRAN Pre-Processor which fully corresponds to a given microstructure (Mishnaevsky et al., 2001a). Other researchers have developed similar programs. For instance, Iung et al. (1996) developed a program which generates FE meshes (to be used by the ABAQUS code) representing the image of a real microstructure. The advantages of this program are that the mesh is generated 'in an iterative way by superimposing on the boundaries square grid of growing size', and is refined automatically at the interfaces between the phases.

In our simulations, we focus on the second approach (automatic generation of FE meshes from microstructure micrographs, and element elimination). Comparison with the first approach (MPE) is carried out as well.

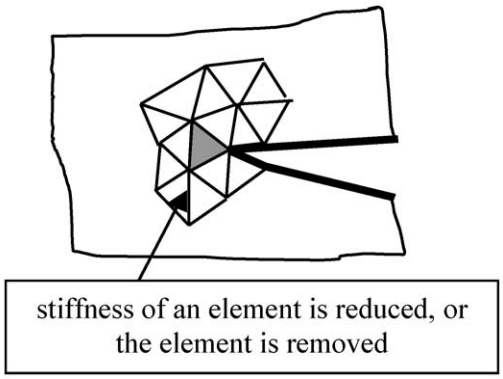

Figure 3. Scheme: Elimination or softening of a finite element.

2.1. Finite element 'softening' and finite element elimination approaches

Among the main numerical approaches to simulating crack growth, the cohesive zone model (Mishnaevsky et al., 1998; Tvergaard and Hutchinson, 1988), smeared crack model (Weihe et al., 1998), representation of cracking by separation of element boundaries (Carter et al., 2000) and the computational cell methodology (Xia et al., 1995; Xia and Shih, 1995) should be mentioned. The separation of element boundaries can be done, for instance, if all the elements in the model, or the elements along the expected crack path present contact elements. According to Broberg's cell model (Broberg, 1997), a material consists of cells (which are defined as the 'smallest material unit that contains reasonably sufficient information about crack growth in the material', and which are characterized by their size and cohesion-decohesion relation). If the cell is considered as an element in a FE mesh, such an approach presents a generalization of cohesive models and the computational cell methodology, developed by Xia et al. (1995) and Xia and Shih (1995).

In our simulations, crack growth is modeled as an elimination of elements in the FE mesh which represents the body. The evident advantages of this approach are that a body may be discretized into simple finite elements (not special contact or interface elements), and that both damage and crack propagation can be modeled in the framework of one and the same local failure condition. Numerically, such element elimination can be realized in two ways: by element 'softening" and by element removal (the last two approaches are often confused) (Mishnaevsky et al., 1999, Mishnaevsky and Schmauder, 2001; Mishnaevsky et al., 2001).

Element 'softening' is done if each element is assumed to be weakened as the local stress or damage parameter exceeds a critical level. The Young's modulus of the elements to be softened is set 1. . .2 orders of magnitude lower than that of the initial material. In some cases, this approach is erroneously called 'element elimination' (Mishnaevsky and Schmauder, 2001). The possibility to model crack growth in such a way is provided by the subroutines UMAT or USDFLD in the ABAQUS FE code.

Another way is to remove the elements from the model, and then to restart the simulation without the eliminated elements, using the RESTART option in ABAQUS.

Figure 3 shows schematically the finite element 'softening' and finite element elimination approaches.

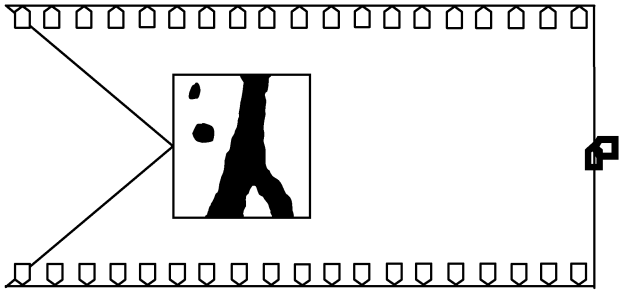

Figure 4. Loading scheme of the mesomodel.

3. Problem statement and FE model

In order to study the effect of the arrangement of inclusions on the fracture resistance of two-phase materials in a systematic way, different idealized microstructures were designed and crack propagation in these microstructures was simulated numerically. The properties of the constituents of the material (particles, matrix) and the expected mechanism of crack growth were determined from in-situ experiments carried out with simultaneous observation of microprocesses in materials in a scanning electron microscope (Mishnaevsky et al., 2003a).

3.1. FE-MODEL

A FE model of short rod specimens was developed (Barker, 1981). The simulations were carried out for 2D plane strain conditions. According to the description of the specimens, the diameter was taken to be 12 mm, height 18 mm, and notch depth 5.32 mm (Barker, 1981). The model consists of a macromodel and a mesomodel. The macromodel was set up in order to determine the displacement distribution on the boundaries of an area 300 μm $\times$ 500 μm in the vicinity of the notch. This area presented then the mesomodel, which included a region with a real steel microstructure. The microstructure of high speed steel was placed in an area 100 μm $\times$ 100 μm near the notch in the model. The displacement distribution on the boundaries of the mesoscopic model was determined from the macromodel. The scheme of the mesomodel and the position of the real microstructure of the steel in the model are shown in Figure 4. The displacement of the points in the vertical direction on the plane of symmetry was set to be zero. The point on the symmetry plane of the specimen, which lies opposite the notch was fixed in the X-direction. Displacement-controlled loading was applied at a point at a distance 1.88 mm from the end of the specimen, according to the real conditions of the loading of short rod specimens. The boundary conditions in the mesomodel (the small area 300×500 μm near the notch of the short-rod-specimen) were given as vertical displacements. The total loading displacement was chosen to be 1 mm. Given properties of the components and the steel, and the real microstructure of the steel, crack initiation and growth in the steel are simulated.

MATERIAL PROPERTIES

The elastic and elasto-plastic properties of the carbides and matrix of the steel were determined using different experimental and experimental-numerical methods, including SEM in-situ experiments (Mishnaevsky et al., 2003a), powder metallurgy production of 'matrix alloy' (Le Calvez et al., 2000), microindentation, etc. The results of the experiments allow us to

Table 2. Mechanical properties of the primary carbides and matrix in high speed steel (Mishnaevsky et al., 2003)

Properties	Carbide	Matrix	Steel	Refs
Young's modulus, GPa	286 (carbides M6C), 351 (MC)	231	240	(Lippman, 1995; Lehmann, 1995; Lippmann et al., 1996)
Poisson's ratio	0.19		0.3	0.3
Local failure criterion	Maximum normal stress	Plastic strain	–	(Mishnaevsky et al., 2001b)
Critical level of the local failure criterion	1500 MPa	0.1%	–	(Mishnaevsky et al., 2001b)
Fracture toughness, K_{Iv}, MPa $m^{1/2}$	–	49	18.9	(Le Calvez et al., 2000)
Constitutive law	Elastic, brittle	$\sigma_y = 1500 + 1101[1 - \exp \epsilon_{pl}/0.00369)]$	$\sigma = 2200 + 820[1 - \exp(-\epsilon_{pl}/0.002)]$	(Le Calvez et al., 2000)

Here: σ_y – von Mises stress, MPa, ϵ_{pl} – plastic strain.

obtain rather comprehensive information about the properties of the constituents of the steel as presented in Table 2.

3.2. Types of ideal microstructures

The purpose of this work is to analyze the effect of the microstructure of steels on the fracture resistance by simulating crack propagation in different microstructures. By testing some typical idealized microstructures in these numerical experiments, factors leading to the optimization and preferable microstructures of materials under given service conditions can be determined.

The ideal microstructures were created with the use of the graphics software XFIG. The particles (primary carbides) are supposed to be round, but their distributions in the microstructure region of the mesomodel were heterogeneous and are varied subsequently. The following types of the particles arrangements were considered:

- band-like microstructures (typical for hot formed steels) and continuous net-like (typical for the cast metals) (Berns, et al., 1997; Mishnaevsky and Schmauder, 1999) (see Figure 5a, c, d),
- random microstructures (see Figure 5b),
- clustered microstructures: the material consists of regions with high and low density of inclusions; these microstructures were studied in (Berns et al., 1998); it was shown in (Berns et al., 1998) that such microstructures ensure a higher fracture resistance, than random or net-like microstructures (see Figure 5e),
- layered microstructures: a material consists of layers with particles of different sizes (see Figure 5f, g, h).

Simple microstructures (random, net-like and band-like) were considered in (Mishnaevsky et al., 2001a, 2003b), and used here only for comparison purposes. In this work, the complex (clustered and layered) microstructures are considered. Two types of clustered microstructures (fine and coarse) were employed (Mishnaevsky et al., 2003b): a fine one with carbide sizes of 2.5 μm and a coarse one with carbide sizes of 3.6 μm. The clustered microstructures contain

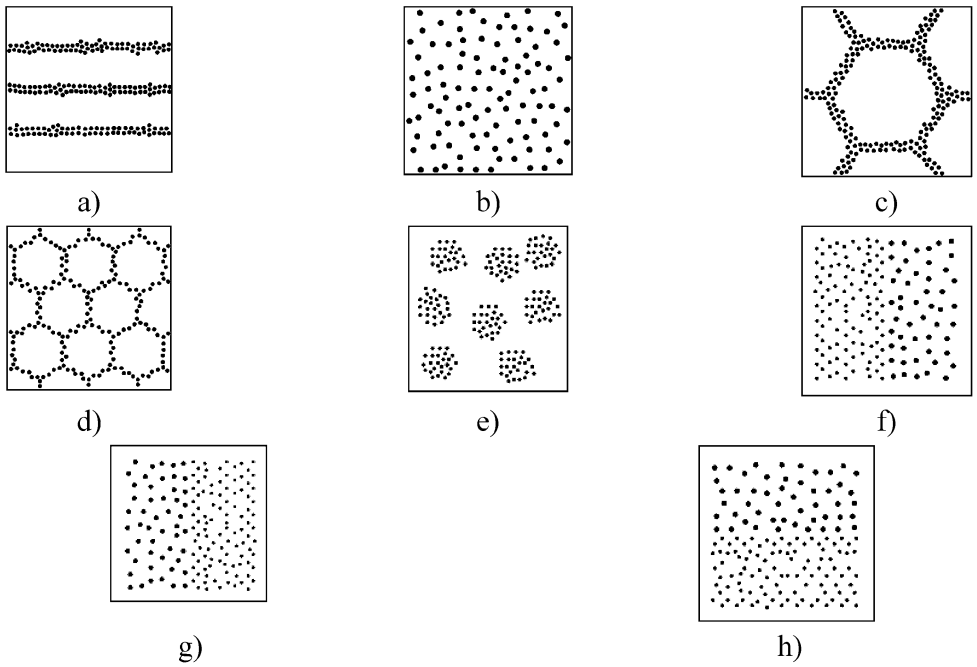

Figure 5. Artificial arrangements of primary carbides considered in this work: (a) band-like, (b) random, (c) net-like coarse, (d) net-like fine (Mishnaevsky et al., 2003b), (e) clustered, (f–h) layered (3 different orientations).

200 carbides of diameter 2.5 μm (fine microstructure) and 100 carbides of diameter 3.6 μm (coarse microstructure), grouped in 8 clusters. The surface content (in this case, volume content) of the particles was about 10% (as for the simple microstructures in (Mishnaevsky, 2003). The layered microstructures were supposed to consist of two layers, one with 100 fine particles (2.5 μm) and another one with 50 coarse particles (3.6 μm). The orientation of the layers as related to the initial notch of the specimen was varied such that the expected mode I crack could go first through a coarse layer and then through a fine layer ('coarse $\rightarrow$ fine structure', Figure 5g), or conversely ('fine $\rightarrow$ coarse structure', Figure 5f), or along the interface between the layers ('coarse/fine structure', Figure 5h).

4. Simulation of crack growth in different microstructures

4.1. Comparison of different numerical techniques

In our simulation, we use program codes for the automatic generation of FE meshes from the micrographs of microstructures. To model damage and crack propagation, we used the element elimination method with RESTART option.

In order to ensure the compatibility of the results from our previous study (crack growth in simple microstructures) and this work, a comparison of the method of a microstructure-based mesh generation with the multiphase element method/element softening was carried out.

The coarse random microstructure from (Mishnaevsky et al., 2003b) was meshed according to both methods: multiphase finite elements (Mishnaevsky et al., 1999) and automatic microstructure-dependent mesh generation (Mishnaevsky et al., 2001a). Then, two different

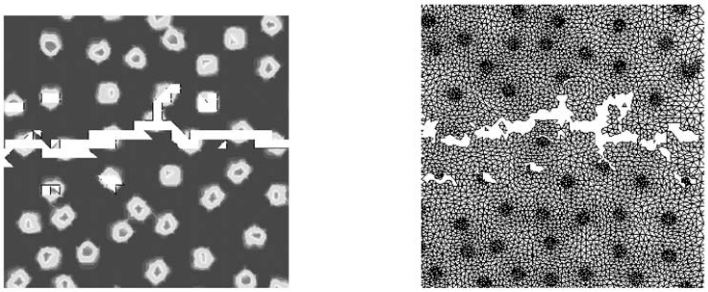

Figure 6. Comparison of the crack path simulated in the artificially designed random coarse microstructure with the use of different numerical approaches: (a) MPE, element softening (Mishnaevsky et al., 2003b), (b) automatically generated FE mesh, element elimination.

Table 3. Quantitative parameters of fracture, determined by two numerical approaches

	1st Method: MPE	2nd Method: microstructure-dependent mesh design
Fracture energy G, J/m	699.18	626.77
Fractal dimension of fracture surface	1.372	1.38
Height of roughness peaks, μm	18	18.6

methods of the simulation of local damage were employed: element softening with relaxation steps and element removal with restarts. Element softening was used in the case of the multiphase elements (since the MPE are used with simple meshes, so the mesh remained intact during the simulation of the crack growth). Element elimination and restarts with new mesh design were employed for the case of the microstructure-based mesh generation.

The crack paths obtained in both cases are shown in Figure 6. Table 3 presents the calculated quantitative parameters of fracture, determined from both simulations. The methods of calculations of the parameters are given below in Section 5.1.

Comparing the results, it can be seen that both quantitative parameters of fracture behavior and qualitative crack path simulated by both methods are almost identical. Thus, it may be expected that the results obtained with the use of these methods are compatible.

4.2. Crack paths in different complex microstructures

Figures 7–10 show the crack paths in the artificial microstructures of the simulated steels. Generally, fracture occurs as follows: first, several carbides fail and form a 'zone of failed carbides' in front of the notch. The 'zone' extends and cracks are formed by coalescence of microcracks in the carbides. Intensive microcracking in carbides before a macrocrack is formed has been observed experimentally as well (Mishnaevsky et al., 2003a).

In the cluster microstructures, the crack grows first in clusters (i.e., it initiates in carbides, and grows from one carbide to another) and then from one cluster to another. Such a mechan-

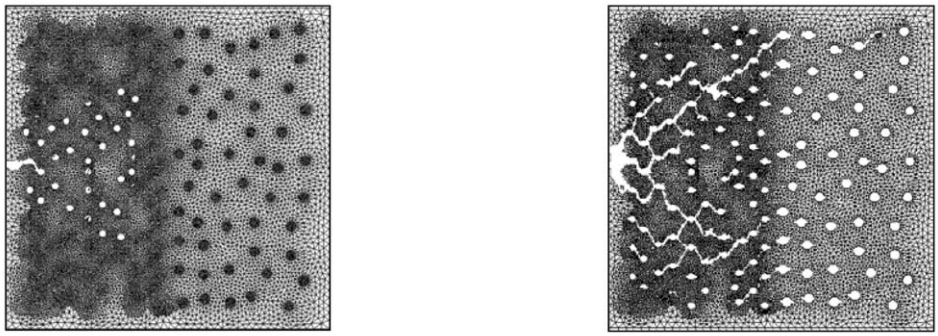

Figure 7. Layered microstructure 1 (fine → coarse): (a) Step 2, u = 6.00E-03 mm and (b) Step 6, u = 7.54E-03 mm.

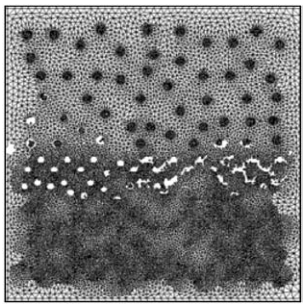

Figure 8. Layered microstructure 2 (coarse/fine): Step 6, u = 7.00E-03 mm.

ism leads to strong deviations of the crack path from its initial direction. In the fine cluster microstructure, two cracks initiated in two different clusters and then propagated by the described mechanism.

In the layered microstructures, crack growth depends strongly on the orientation of the layers: in the 'coarse-fine' microstructure, a large crack forms at the initial stage of loading, and propagates first straightforward and then at an angle of about 45 degree with respect to the initial direction. Crack deflection and branching is especially strong in the fine layer. In

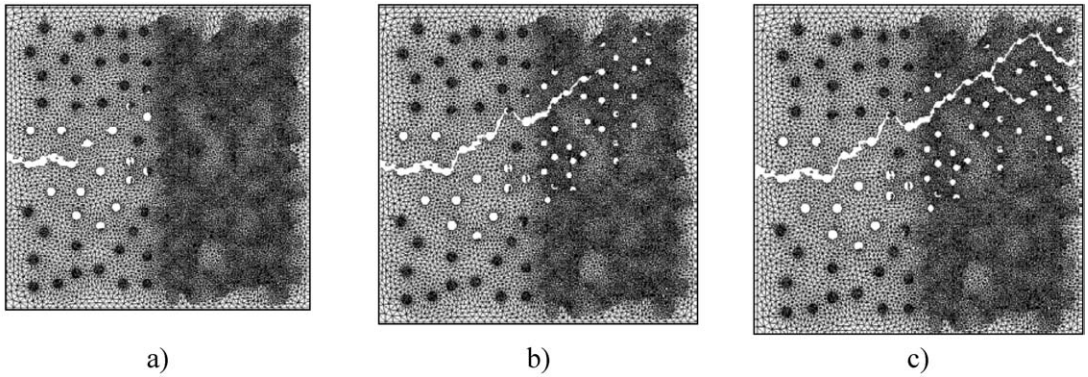

Figure 9. Layered microstructure 1 (coarse → fine): (a) Step 8, u = 6.38E-03 mm, (b) step 14, u = 6.75E-03 mm, (c) step 26, u = 7.13E-03 mm.

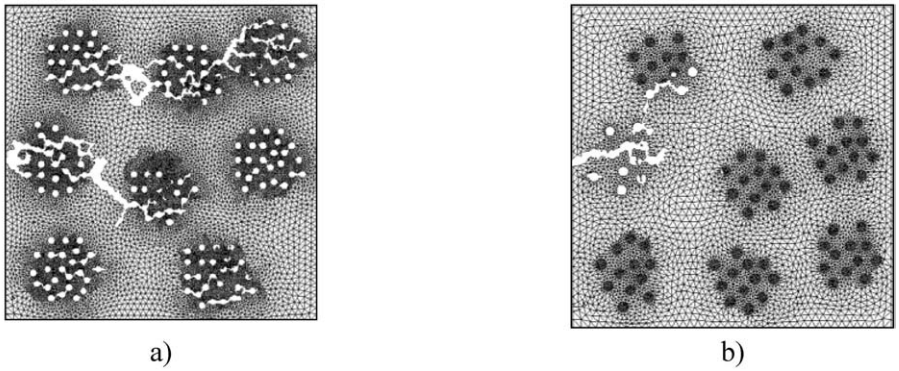

Figure 10. Cluster microstructures: (a) Fine, step 6, u = 5.99E-03 mm, (b) Coarse, step 6.

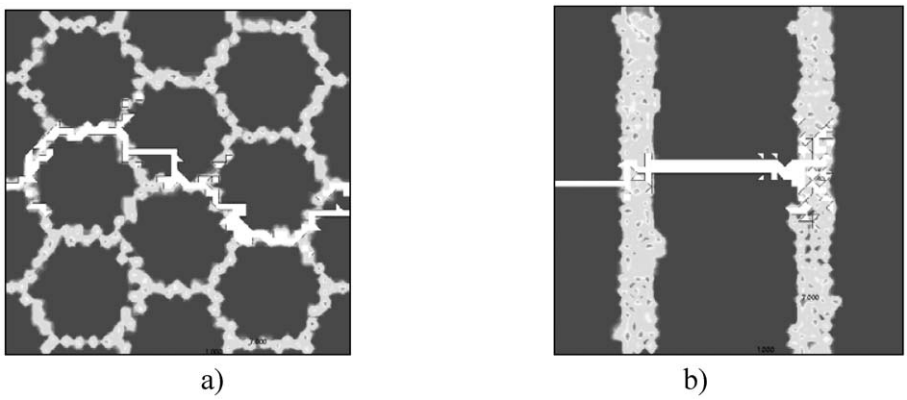

Figure 11. Crack path in net-like microstructures (a) and band-like microstructure (b) (given here for comparison purposes) (Mishnaevsky et al., 2003b).

the 'finecoarse' microstructure, the 'zone of failed carbides' propagates rather far away from the crack tip, but only a small macrocrack forms in that zone (no coalescence of microcracks formed in the carbides). After the microcracks in the large 'zone of failed carbides' coalesce, crack with many branches forms. In the 'coarse/fine' microstructure (which is in fact symmetric relatively to the notch), the crack grows in the layer of fine carbides, rather than in the layer of coarse carbides: the carbides fail in the layer of fine carbides, and the 'zone of failed carbides' extends in the fine layer. When the 'zone' becomes large enough, the microcracks coalesce and macrocracks form. However, no such zone and no cracks form in the area of coarse carbides: after the failure of few carbides near the notch, damage growth in the layer of coarse carbides stops. Apparently, the longer distances between primary carbides (potential microcrack initiation sites) in the coarse part prevent the microcracks from joining together in the coarse structures, but not in the layer of fine carbides.

Crack paths in complex structures were compared with those in simple microstructures obtained in (Mishnaevsky et al., 2003b): In the fine net-like microstructure (Figure 11a), the crack is instantly directed to the carbide network, and then follows exclusively the carbide network. Such a mechanism ensures maximum fracture resistance of the steel (see Section 5.1). In the band-like (Figure 11b) and coarse net-like structure, the crack grows rectilinearly in the matrix, and undergoes notable deflections at the carbide bands.

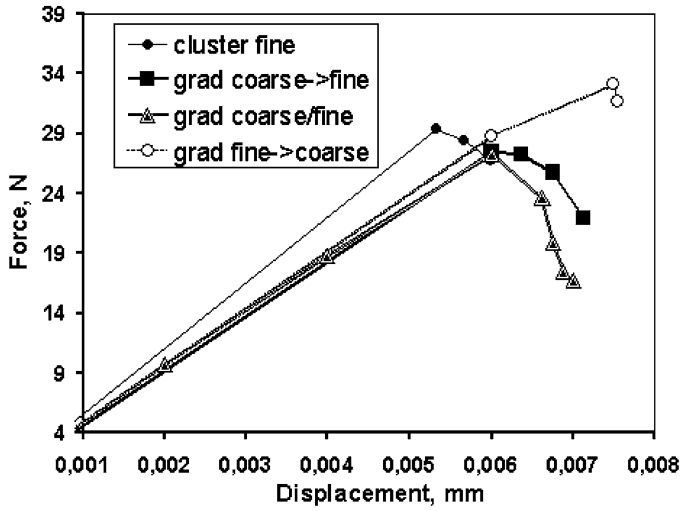

Figure 12. Force-displacement curves for the simulated microstructures.

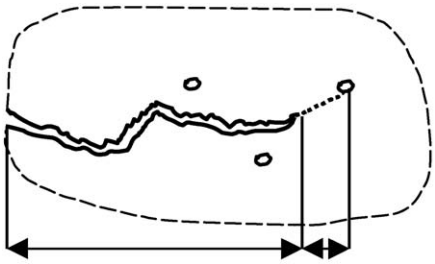

Figure 13. Scheme: Crack path variations due to the microcracks.

5. Comparison of different types of microstructures

5.1. Fracture resistance of the materials with artificial microstructures

For all simulations performed, the force-displacement curves, energy and geometrical parameters were determined numerically. Figure 12 shows the force-displacement curves for the simulated microstructures.

Table 4 provides some main quantitative characteristics of crack growth in the different structures. The value of G (nominal specific energy of the formation of a unit of new surface) for each microstructure characterizes the fracture resistance of each of the structures. This value was calculated as follows: $G = \sum_i (P_i u_i)/BL_{RS}$, where P_i – force for loading step, u_i – displacement for loading step i, L_{RS} – linear size of the real microstructure in the horizontal direction, the summation is carried out for all i loading steps until the crack passes the real microstructure, B – the thickness of the model (Mishnaevsky et al., 2003b).

To characterize crack, we consider the maximal height of the roughness peak R_{max}, the number of eliminated elements not connected to the main crack as well as branches of the crack, and the fractal dimension of the crack. The maximal height of the roughness peak R_{max} was calculated from the crack profile as the distance between highest and lowest points of the crack path measured perpendicular to the initial horizontal crack direction.

Table 4. Quantitative parameters of fracture behavior of the artificial structures of steels

	Complex structures				Simple structures (from Mishnaevsky et al., 2003)		
	Layered			Cluster	Net-like*	Band-like*	Random*
	'C→F'	'C→C/F'	'F→C'	fine			
Nominal specific energy of new surface, J/m^2	668.9	786.1	733.9	635.7	436.15/827.0	341.28/676.75	699.18/557.02
Maximal height of the roughness peak, R_{max}, μm	44	46	44	35	13/36	24/14	18/12
Fractal dimension of fracture surface, D	1.522	1.556	1.382	1.515	1.285/1.593	1.442/1.40	1.372/1.446

*The values are given for coarse/fine versions of the microstructure, respectively.

The fractal dimension of the fracture surface was calculated on the basis of following considerations. Cracks grow both in reality, and in our simulation by joining microcracks (in our model by joining softened or removed finite elements). The removed elements lie in front of the crack tip but not necessarily in the plane of straight mode I crack propagation. The joining of elements, which do not lie in the plane of crack propagation causes random variations of the direction of crack growth (see Figure 13), and these variations determine the fractal dimension D of a fracture surface (Mishnaevsky, 1996; 1998: Xie, 1993), similarly to the formation of a fractal cluster from randomly moving particles (Mishnaevsky, 1998). For a fractal cluster which grows by such a mechanism, the fractal dimension of a cluster is given by the formula: $i \propto L^D$, where i – the number of particles (in our case, the number of unit steps L of the crack growth, or eliminated finite elements), L – projected crack length. To determine the fractal dimension D of the crack path from the above simulations, the number of eliminated elements and the projected length of the crack after each loading step are determined, and the power in the i-L-relationship for each of the structures is calculated. One should note here that the fractal dimensions calculated with the use of this method present just rough estimations. In order to determine the fractal dimension of a crack more exactly, simulations of longer crack growth in much bigger microstructure samples should be carried out. This will be the subject of future investigations.

For comparison purpose, the results for the simple microstructures from (Mishnaevsky et al., 2003b) are given in the Table 4 as well.

Figure 14 shows the fractal dimension plotted versus the fracture energy. One can see that the fracture energy increases with increasing fractal dimension of fracture surface.

Figure 15 shows a comparison of the fracture resistances of the different microstructures. From the figure it can be seen that the heterogeneous microstructures with localized brittle particle distributions (i.e., clustered and layered ones) ensure rather high fracture resistances (Mishnaevsky and Shioya, 2001). This can be explained by the fact that these microstructures lead to strong crack deviations: from one region of high particle density to another one (in a clustered microstructure) or in the layer of fine particles. The fracture resistances of the microstructures with spatially localized particle arrangements are always higher than those of

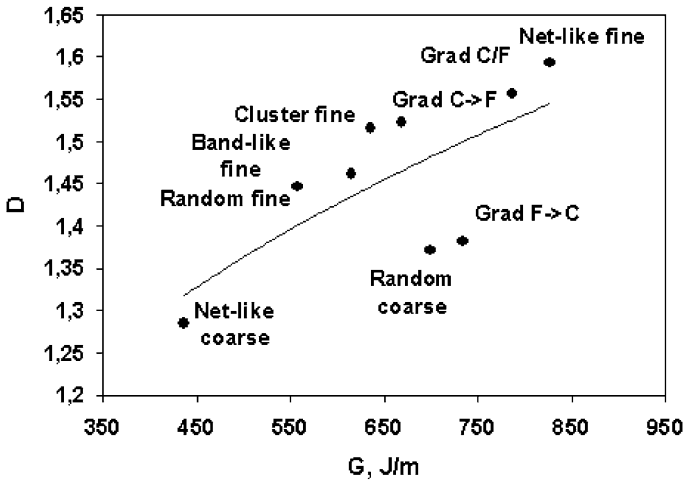

Figure 14. Fractal dimension D plotted versus the calculated fracture energy.

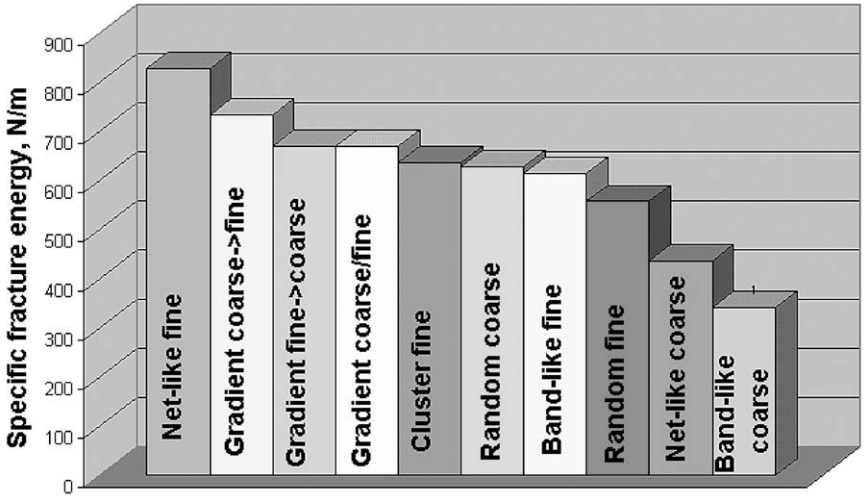

Figure 15. Comparison of fracture resistance of different artificial microstructures.

simple microstructures, except for the case of the net-like fine microstructure. In the net-like structure, the crack is forced to follow the carbide network, and the crack path becomes much longer than the mode I crack path. This ensures a rather high fracture resistance. However, this toughening mechanism is unstable, since the crack propagates through the carbide network when the network cells are big enough resulting in a very low fracture toughness.

Table 5 summarizes the assessments for fracture toughness and mechanisms of toughening for different structures.

5.2. Crack deflection and the fatigue behavior of the crack

Now we estimate the change in the fatigue crack behavior caused by microstructure-induced crack deflections following the model of Suresh (1998), assuming that the crack paths in the case of monotonic loading and cyclic loading are similar. According to Suresh (1998), the

Table 5. Assessment of artificial microstructures

Type	Peculiarities of the mechanism	Mechanism of toughening
Net-like	Crack follows the carbide network. However, this toughening mechanism is unstable: if the cells are too large, the crack propagates through the cells.	Crack path (determined by the carbide network) is much longer than without the network
Bandlike	Crack jumps from one band to another and deflects at the bands.	Crack path deviations at the bands; high toughness of the matrix between bands.
Random	Crack jumps from one carbide to another.	Intensive crack branching and damage formation also apart from the crack path
Layered	A. 'coarse → fine': carbides fail in coarse layer, but a crack forms only at high K_I. The fine layers lead to strong deviations of crack direction from the initial path. B. '$\frac{\text{coarse}}{\text{fine}}$': the crack preferably grows in the fine layer, rather than in the coarse layers	Crack path deviations in the layer of fine particles; high toughness of the matrix between the particles.
Clustered	Crack grows first in clusters (jumps from one carbide to another) and then from one cluster to another.	Crack path deviations from the initial direction due to the jumps to nearest clusters

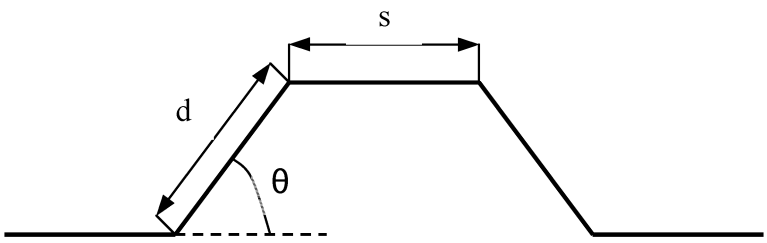

Figure 16. Schematization of the crack deviation according to Suresh (1998).

apparent crack propagation rate (i.e., measured along the mode I crack direction) changes due to the crack deviations as:

$$v/v_L \sim m \cos\theta + (1 - m), \tag{1}$$

where v_L is the growth rate of a straight crack under the same loading conditions as the kinked crack, θ is the kink angle, $m = 1/(1 + s/d)$, d – distance over which the tilted crack advances along the kink, and s is the distance over which the plane of the growing crack is normal to the far-field tensile axis (see Figure 16).

Table 6 gives the value of θ, d, s and m for the cracks simulated above.

From Table 6, it can be seen that the maximum estimated reduction of the crack rate due to the crack deflection is observed in the layered 'fine→coarse' and 'coarse→fine' microstructures, i.e. on the structures where one of the layers forces the intensive crack kinking and branching. Comparing the values of fractal dimension of the fracture surface (given in Table 4) and the values of the relative reduction of crack rate v/vL, it may be seen that the higher values of fractal dimension and roughness of the crack surface correspond to a stronger

Table 6. Coefficients of the formula for the reducing fatigue crack growth rate

Type of microstructures	Kink angle θ	Distance d (tilted)	Distance s (straight)	Coefficient m	Coefficient v/v_L
Layered fine → coarse	∼32	46	47	0.515	0.014
Layered coarse/fine	∼30	14	5.7	0.710	0.88
Layered coarse→fine	∼45	20	14.8	0.574	0.07
Cluster coarse	∼80*	10.6	27	0.281	0.63
Cluster fine	∼20*	27	28	0.49	0.036

*Crack kinks from the end of a cluster to the next cluster.

reduction of the crack growth rate due to deviations of crack path from the mode I direction of crack growth.

Further works include the experimental verification of the numerical conclusions as well as carrying out the FE simulations of the propagation of long cracks in greater volumes of material, as compared with the above simulations. The simulations of large crack growth may allow to use some finer method of the calculation of the fractal dimension (Mishnaevsky, 1997, 1998; Xie, 1993), as the simple method used above.

6. Conclusions

On the basis of our numerical investigations, the fracture mechanisms in the materials with different arrangements of brittle round inclusions were clarified.

Clustered and layered heterogeneous microstructures ensure rather high fracture resistances, which are always higher than those of simple microstructures, i.e. band-like, net-like or random ones. This is determined by the fact that these heterogeneous microstructures lead to strong crack deviations: from a region of high particle density to another one (in the clustered microstructure) or into the layer of fine particles.

Net-like fine microstructure shows an exception to this rule and forces the crack to follow the carbide network, ensuring the highest fracture resistance, even higher than all the complex microstructures. However, such a mechanism of toughening is unstable: the net-like coarse microstructure (with larger cells) provides very low fracture toughness, since the crack propagates in a straight manner rather than following the carbide network.

The investigations lead to the conclusion that complex (clustered and layered) microstructures possess the potential for improving the fracture toughness of steels. The main mechanisms of the positive toughening effect by complex microstructures are identified: crack path deviations from its initial direction (which increase the crack length without increasing the stress intensity factor K_I), and large areas of the tough matrix between the areas of high inclusion density.

Acknowledgements

One author (LM) is grateful to the Deutsche Forschungsgemeinschaft for its support via the Heisenberg Fellowship (project DFG MI 666/4-1 '*Optimization of Materials at the Mesolevel on the Basis of Numerical Experiments taking into Account the Effects of heterogeneous, complex and hierarchical Microstructures*'). The authors gratefully acknowledge the financial support by the Deutsche Forschungsgemeinschaft via the project DFG Schm-746/30-1 '*Optimization of High Speed Steels by Varying their Microstructures on the basis of the Fractal Analysis of Interrelations between the Microstructure and Fracture*'.

References

Barker, L.M. (1981). Short Rod and Short Bar Fracture Toughness Specimen Geometries and Test Methods for Metallic Materials. *Fracture Mechanics ASTM STP* **743**, 456–475.

Berns, H., Broeckmann, C. and Weichert, D. (1997). Fracture of Hot Formed Ledeburitic Chromium Steels. *Engineering Fracture Mechanics* **58**(4), 311–325.

Berns, H., Melander, A., Weichert, D., Asnafi, N., Broeckmann, C. and Gross-Weege, A. (1998). A new material for cold forging tool. *Comput Mater Sci* **11**, 166–180.

Broberg, K.B. (1997). The Cell Model of Materials. *Computational Mechanics* **19**(7), 447–452.

Broeckmann, C. (1994). Bruch karbidreicher Stähle – Experiment und FEM-Simulation unter Berücksichtigung des Gefüges, Dissertation, Ruhr-Universitaet Bochum.

Carter, B.J., Wawrzynek, P.A. and Ingraffea, A.R. (2000). 'Automated 3D Crack Growth Simulation' Gallagher Special Issue of Int. J. Num. Meth. Engng. Vol. 47, pp. 229–253.

Gross-Weege, A. Weichert, D. and Broeckmann, C. (1996). Finite Element simulation of crack initiation in hard two-phase materials. *Comput Mat Sci* **5**, 126–142.

Iung, I., Petitgand, H., Grange, M. and Lemaire, E. (1996). Mechanical behaviour of multiphase materials Numerical simulations and experimental comparisons, Proc IUTAM Symposium on Micromechanics of Plasticity and Damage in Multiphase Materials, Kluwer, 99–106.

Le Calvez, Ch., Ponsot, A., Mishnaevsky, L. Jr., Iturizza, I., Rodriguez Ibabe, J.M., Lichtenegger, G. and Schmauder, S. (2000). Micromechanical Mechanisms of Strength and Damage of Tool Steels under Static and Cyclic Loading, CLI, Le Creusot, France. Final Reports on ECSC RTD Project.

Lippmann, N., Lehmann, A., Steinkopff, Th. and Spies, H.-J. (1996). Modelling the Fracture Behaviour of High Speed Steels under Static Loading. *Comp. Mat. Sci.* **7**, 123–130.

Lehmann, A. (1995). Modellierung des Bruchverhaltens von Schnellarbeitsstählen unter Beachtung bauteilspezifischer Einflüsse, Diplomarbeit, TU Bergakademie Freiberg.

Lippmann, N. (1995). Beitrag zur Untersuchung des Bruchverhaltens von Werkzeugen aus Schnellarbeitsstählen unter statischer Beanspruchung, Dissertation, Freiberg.

Mishnaevsky Jr., L. (1996). Determination for the Time to Fracture of Solids. *Int. J. Fracture* **79**(4), 341–350.

Mishnaevsky Jr., L. (1997). Methods of the Theory of Complex Systems in Modelling of Fracture: a Brief Review. *Eng. Fract. Mech.* **56**(1), 47–56.

Mishnaevsky Jr., L. (1998). *Damage and fracture of heterogeneous materials*. Balkema, Rottterdam.

Mishnaevsky Jr., L. and Schmauder, S. (1999a). SEM-in-situ- Experiments on the Deformation and Fracture of Cold Work and High Speed Steels, Report for Boehler Edelstahl GmbH, MPA, 1999, 35 p.

Mishnaevsky Jr., L. and Schmauder, S. (1999b). Optimization of Fracture Resistance of Ledeburitic Tool Steels: a Fractal Approach 'Steels and Materials for Power Plants'. (Edited by P. Neumann et al.), Proceedings of EUROMAT-99 (European Congress on Advanced Materials and Processes, Munich), Vol. 7, Wiley-VCH Verlag, Weinheim.

Mishnaevsky Jr., L. and Schmauder, S. (2001). Continuum Mesomechanical Finite Element Modeling in Materials Development: a State-of-the-Art Review. *Applied Mechanics Reviews* **54**(1), 49–69.

Mishnaevsky Jr., L. and Shioya, T. (2001). Optimization of Materials Microstructures: Information Theory Approach, Journal of the School of Engineering, The University of Tokyo, Vol. 48, pp. 1–13.

Mishnaevsky Jr., L., Dong, M., Hoenle, S. and Schmauder, S. (1999). Computational Mesomechanics of Particle-Reinforced Composites. *Comp. Mater. Sci.* **16**(1–4), 133–143.

Mishnaevsky Jr., L., Lippmann, N. and Schmauder, S. (2000). Mesomechanical Simulation of Crack Propagation in Real and Quasi-Real Idealized Microstructures of Tool Steels, Proc. 13th European Conference on Fracture 'Fracture Mechanics: Applications and Challenges', 6th – 9th September, San Sebastián, Spain, CD-ROM.

Mishnaevsky Jr., L. Lippmann, N. and Schmauder, S. (2001a). Computational Design of Multiphase Materials at Mesolevel, ASME International Mechanical Engineering Congress and Exposition, November 11-16, New York, CD-ROM Proceedings, Vol. 2.

Mishnaevsky Jr., L. Lippmann, N. and Schmauder, S. (2001b). Experimental-Numerical Analysis of Mechanisms of Damage Initiation in Tool Steels, Proc. 10th International Conference Fracture, 3-7 Dec Honolulu, USA, CD-ROM.

Mishnaevsky Jr., L., Weber, U., Lippmann, N. and Schmauder, S. (2001c). Computational Experiment in the Mechanics of Materials, 'Computational Modeling of Materials, Minerals, and Metals Processing', Proceeding TMS Conference, Eds. M. Cross, J.W. Evans, and C. Bailey, pp. 673–680.

Mishnaevsky Jr., L. Lippmann, N. and Schmauder, S. (2003a). Micromechanisms and Modelling of Crack Initiation and Growth in Tool Steels: Role of Primary Carbides. *Zeitschrift f. Metallkunde* (Int. J. Materials Research) **94**(6), 676–681.

Mishnaevsky Jr., L., Lippmann, N. and Schmauder, S. (2003b). Computational Modeling of Crack Propagation in Real Microstructures of Steels and Virtual Testing of Artificially Designed Materials. *International Journal of Fracture* **120**(4), 581–600.

Mishnaevsky Jr., L. Mintchev, O. and Schmauder, S. (1998). FE-Simulation of Crack Growth Using a Damage Parameter and The Cohesive Zone Concept, In: 'ECF 12 - Fracture from Defects', Proc. 12th European Conference on Fracture (Sheffield, 1998). Eds. M.W. Brown, E.R. de los Rios and K. J. Miller. London, EMAS, Vol. 2, pp. 1053–1059.

Plankensteiner. A.F., Böhm, H.J., Rammerstorfer, F.G. and Buryachenko, V.A. (1996). Hierarchical modelling of high speed steels as layer-structured particulate MMCs, J de Physique IV, 6, 395–402.

Plankensteiner, A.F., Böhm, H.J., Rammerstorfer, F.G. and Pettermann, H.E. (1998). Multiscale modelling of highly heterogeneous particulate MMCs, Proc 2nd Europ Conf Mechanics of Materials, Magdeburg, 291–298.

Schmauder, S. and Mishnaevsky, L. (2001). Damage in Metallic Multiphase Materials: Mechanisms and Mesomechanics, MPA Stuttgart, Preprint, 110 pp.

Suresh, S. (1998). *Fatigue of Materials*. Cambridge University Press.

Tvergaard, V. and Hutchinson, J.W. (1988). Effect of T-Stress on Mode I Crack Growth Resistance in a Ductile Solid. *Int. J. Solids Struct.* **31**(6), 823–833.

Weihe, S., Kröplin, B. and de Borst, R. (1998). Classification of Smeared Crack Models Based on Material and Structural Properties. *Int. J. Solids and Structures* **35**(12), 1289–1308.

Xia, L. and Shih, C.F. (1995). Ductile crack growth - II. Void nucleation and geometry effects on macroscopic fracture behavior. *J. Mech. Phys. Solids* **43**(11), 1953–1981.

Xia, L., Shih, C.F. and Hutchinson, J.W. (1995). A computational approach to ductile crack growth under large scale yielding conditions. *J. Mech. Phys. Solids* **43**(3), 389–413.

Xie, H. (1993). *Fractals in Rock Mechanics*. Balkema, Rotterdam.